Chapter 7

Comparison of the Laminar Flat Flame Dynamics of Methane, Propane and Ethane Combustion

Chapter 6 contained a detailed description of the results of the dynamic experiments conducted with burning methane, propane and ethane. The experimental results were analyzed and correlated to key physical parameters to gain a better insight of the dominant dynamic processes occurring in laminar flat flames. One of the most significant conclusions was that chemical kinetics and the flame speed oscillations dominated the dynamics of burner stabilized laminar flat flames in the bandwidth of 30 to 250 Hz. Both these parameters are very much fuel dependent. Since natural gas is primarily a mixture of methane, ethane and propane, changes in its composition are expected to effect the dynamic characteristics of the combustion process. Therefore, it is essential to compare the dynamics results of methane, ethane and propane flames, and draw conclusions as to how the variations in the composition of natural gas will effect the occurrence of thermo-acoustic instabilities.

7.1 Comparison of Experimental Results

7.1.1 Flow Rate Variation at Ultra Lean Conditions

Figure 7.1 through Figure 7.6 show the FRF magnitude and the FRF phase of the three fuels at $\Phi = 0.55$ and Q_{Total} of 160 cc/sec, 180 cc/sec, and 200 cc/sec. Comparing the magnitude of the FRF for the three flow rates, it is noted that propane flames always have a significantly higher dynamic gain than methane flames in the frequency range of 20-100 Hz. The difference in the dynamic gain is at least 10 dB in general and at certain conditions it is as high as 15 dB. Beyond 100 Hz, the difference in the dynamic gain is reduced to about 3 dB for the flow rates of 160 cc/sec and 180 cc/sec, but it is around 5 dB for the flow rate of 200 cc/sec.

On the other hand, ethane flames exhibit a lightly damped peak in the frequency range of 30-60 Hz, due to the close proximity of the two resonant poles. This character is responsible for the highest dynamic gain demonstrated by ethane flames (15 to 18 dB more than the dynamic gain of methane flames), in a narrow low frequency bandwidth. At $Q_{Total} = 160$ cc/sec, the high gain bandwidth for ethane flames is 35-60 Hz. This band broadens to 20-100 Hz for the flow rate of 200 cc/sec. However, at higher frequencies ethane flames exhibit at least a 5 dB lower gain than methane flames.

Comparing the phase of the FRF of the three fuels, it is noted that the 1^{st} resonant response of ethane flames is the least damped, while that of methane flames is the most damped. This is concluded because the rate of decrease of phase around the resonant frequencies is the highest for ethane flames and lowest for methane flames. For low flow rates and for frequencies less than 100 Hz, the phase of both the ethane and propane flames lags behind that of methane flames, while for frequencies greater than 100 Hz, the difference in phase between the three fuels is narrowed down to less than 15 degrees. With increase in total flow rate, there is a measurable difference in the phase of the three fuels over the entire bandwidth of 20-380 Hz. Under all conditions, ethane flames exhibit the greatest deviation

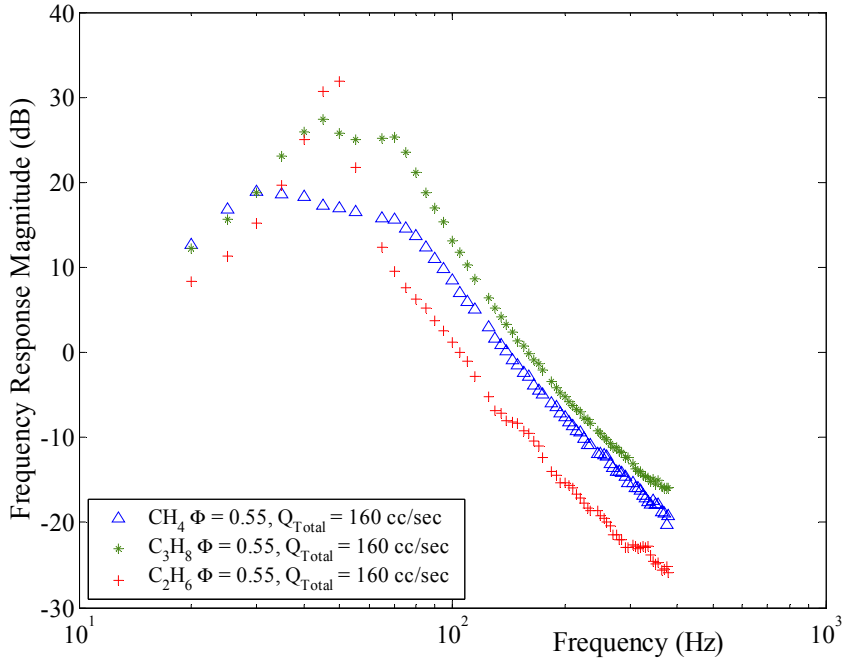

Figure 7.1: FRF (magnitude) for $Q_{Total} = 160$ cc/sec and $\Phi = 0.55$

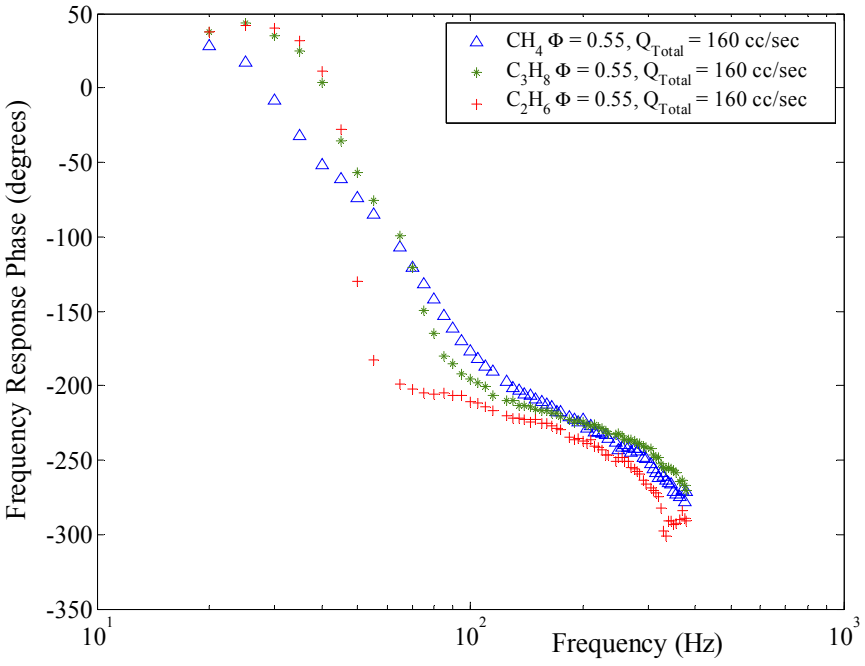

Figure 7.2: FRF (phase) for $Q_{Total} = 160$ cc/sec and $\Phi = 0.55$

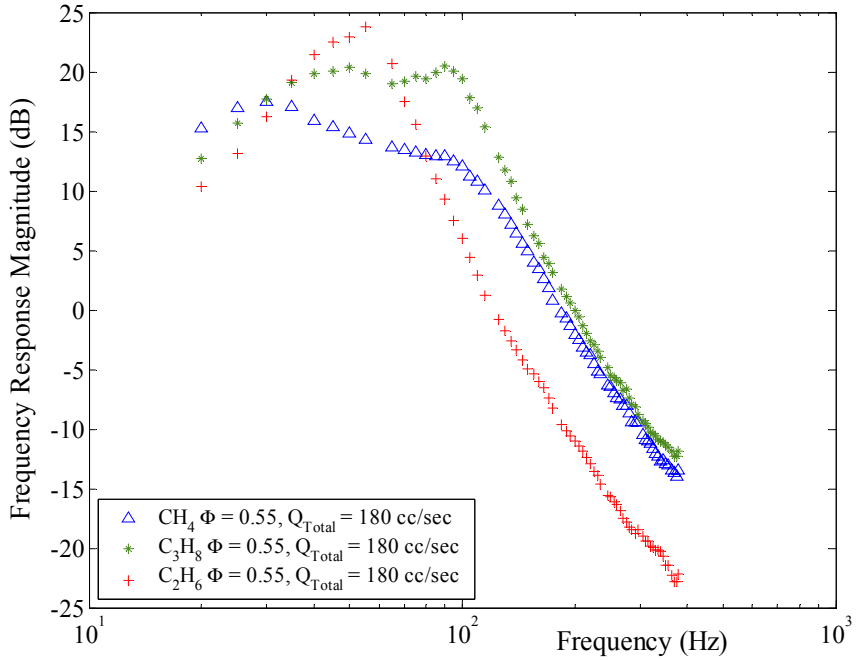

Figure 7.3: FRF (magnitude) for $Q_{Total} = 180$ cc/sec and $\Phi = 0.55$

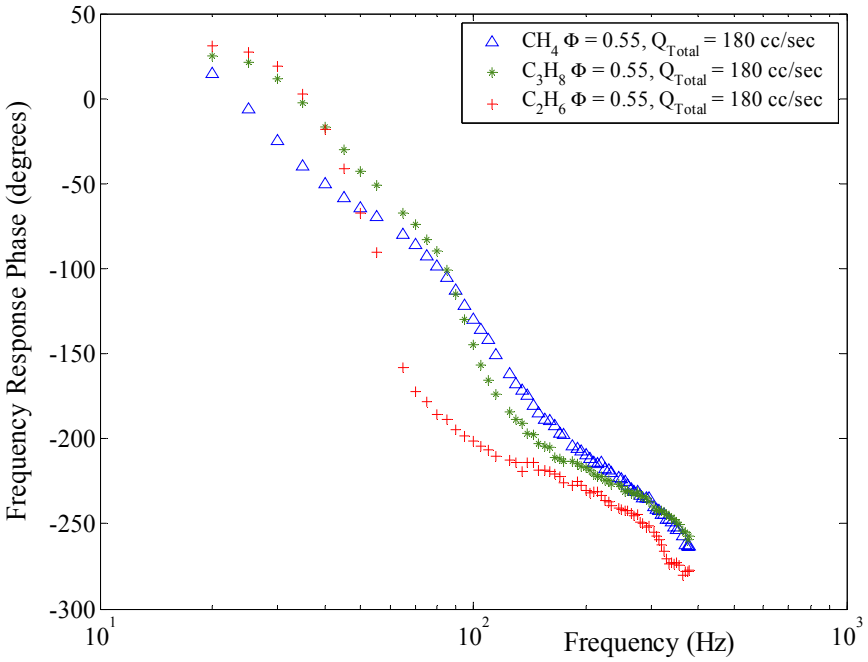

Figure 7.4: FRF (phase) for $Q_{Total} = 180$ cc/sec and $\Phi = 0.55$

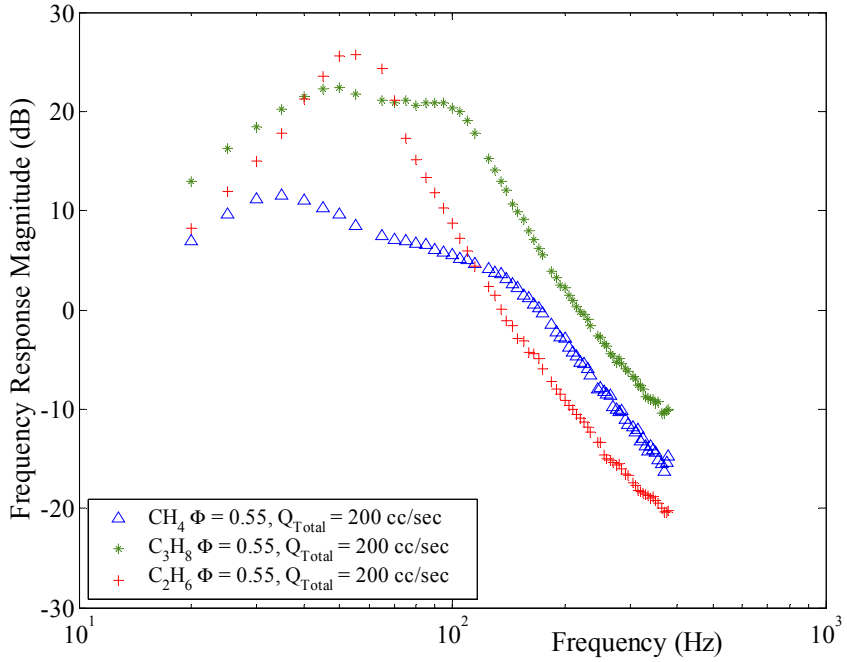

Figure 7.5: FRF (magnitude) for $Q_{Total} = 200$ cc/sec and $\Phi = 0.55$

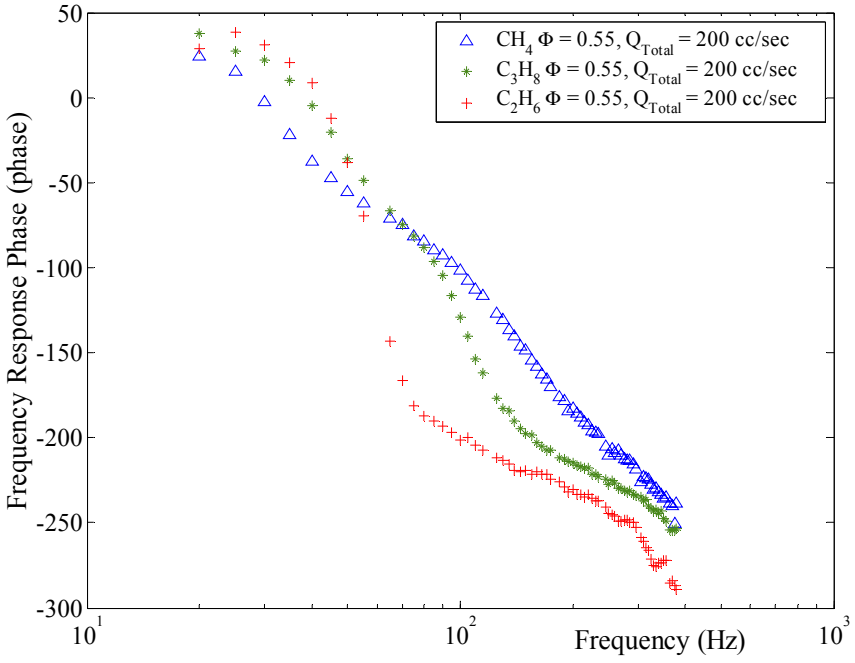

Figure 7.6: FRF (phase) for $Q_{Total} = 200$ cc/sec and $\Phi = 0.55$

in phase from the methane flames.

The observations described above indicate that for ultra lean conditions, burning of propane instead of methane increases the likelihood of thermo-acoustic instabilities, as propane increases the dynamic gain in the system and also effects the phase characteristics. Thus, marginally stable systems burning methane at very low Φ will almost certainly exhibit thermo-acoustic instabilities upon switching to propane. Burning of ethane instead of methane in flames that are stabilized at ultra lean conditions is expected to lower the dynamic gain in the system at frequencies greater than 100 Hz and in most cases increase the dynamic gain in the system for frequencies below 100 Hz. The change in phase caused by switching to ethane will almost certainly shift the phase cross over frequencies of the closed loop combustion system. Thus, stable or marginally stable systems could exhibit instabilities at some other frequency. On the other hand, depending on the dynamic characteristics of the closed loop combustion process, burning ethane could have a stabilizing effect.

7.1.2 Effect of Increase in Equivalence Ratio

Figure 7.7 through Figure 7.14 show the FRF magnitude and the phase of the dynamic response for flames with the three fuels for $\Phi = 0.65$ and $\Phi = 0.75$, and Q_{Total} of 145 cc/sec and 200 cc/sec. Evaluating these figures along with Figure 7.1 through Figure 7.6, it is observed that an increase in Φ from 0.55 to 0.75 causes the dynamic gain of ethane to become almost equal to that of methane for all the frequencies. However, there are intermediate conditions such as $\Phi = 0.65$ where ethane flames exhibit a greater gain than methane flames by about 3 dB over a wide bandwidth of 35 to 180 Hz. The large difference in the phase of ethane and methane flames observed at low Φ almost vanishes as Φ increases and for $\Phi = 0.75$, the phase of both flames is almost identical. On the other hand, comparing propane and methane flames, at $\Phi = 0.55$ propane flames exhibit a significantly higher gain of 10-15 dB at low frequencies, which diminishes to 3 dB at higher frequencies. As Φ increases, propane flames show a dynamic gain of about 5 db greater than that of methane flames over

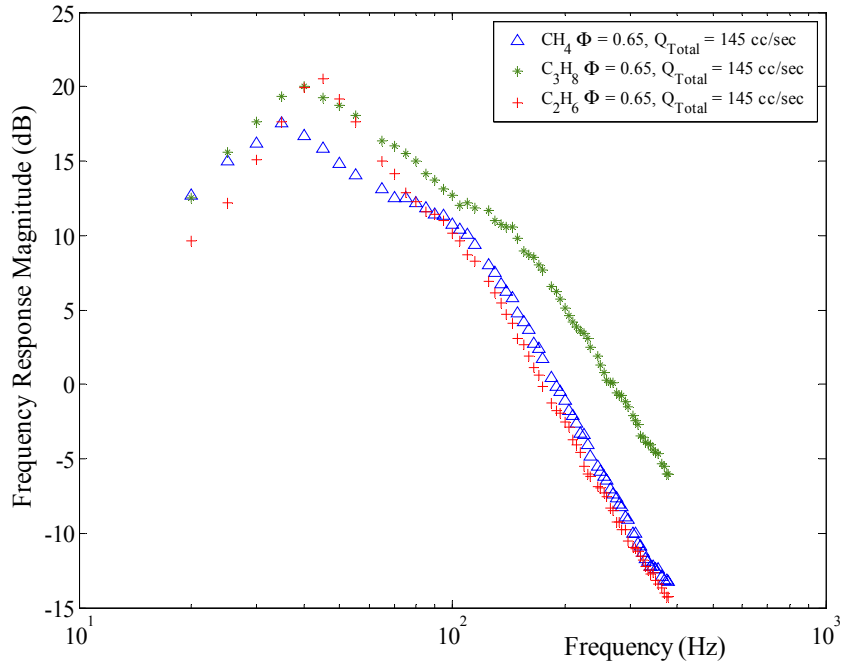

Figure 7.7: FRF (magnitude) for $Q_{Total} = 145$ cc/sec and $\Phi = 0.65$

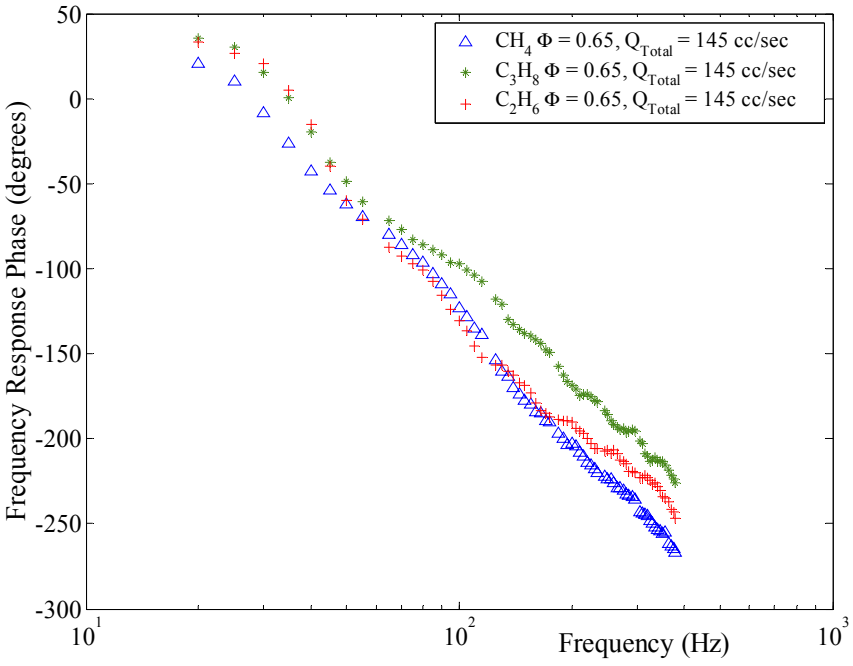

Figure 7.8: FRF (phase) for $Q_{Total} = 145$ cc/sec and $\Phi = 0.65$

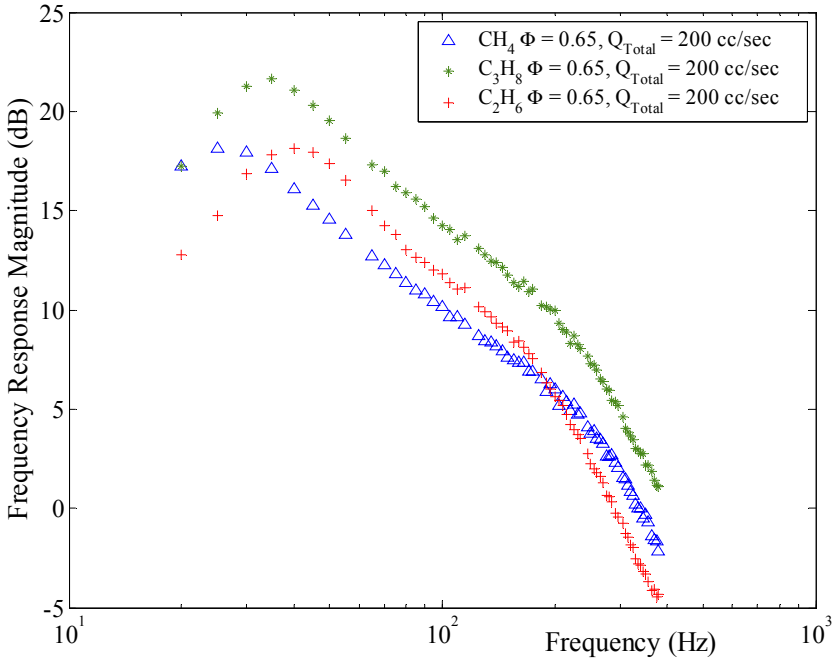

Figure 7.9: FRF (magnitude) for $Q_{Total} = 200$ cc/sec and $\Phi = 0.65$

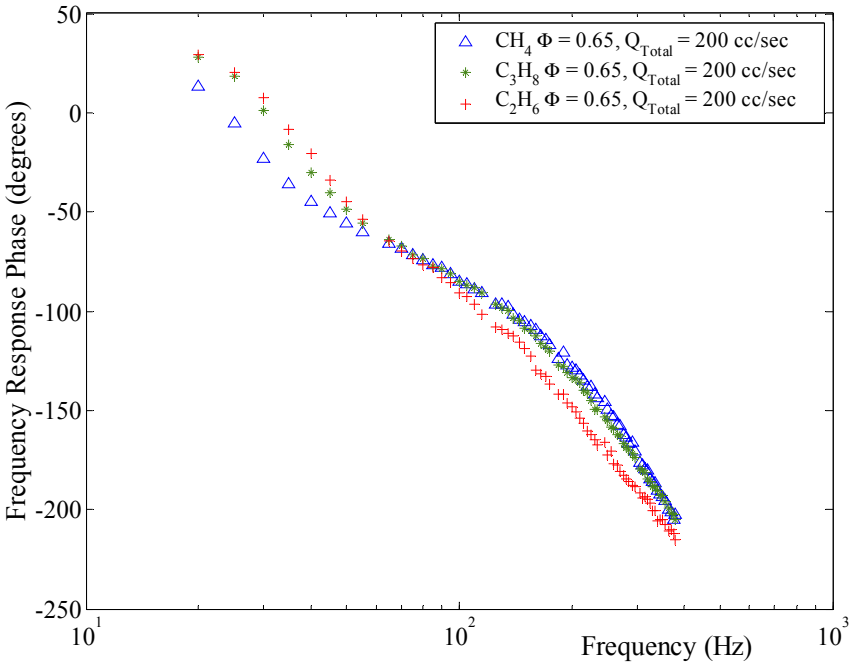

Figure 7.10: FRF (phase) for $Q_{Total} = 200$ cc/sec and $\Phi = 0.65$

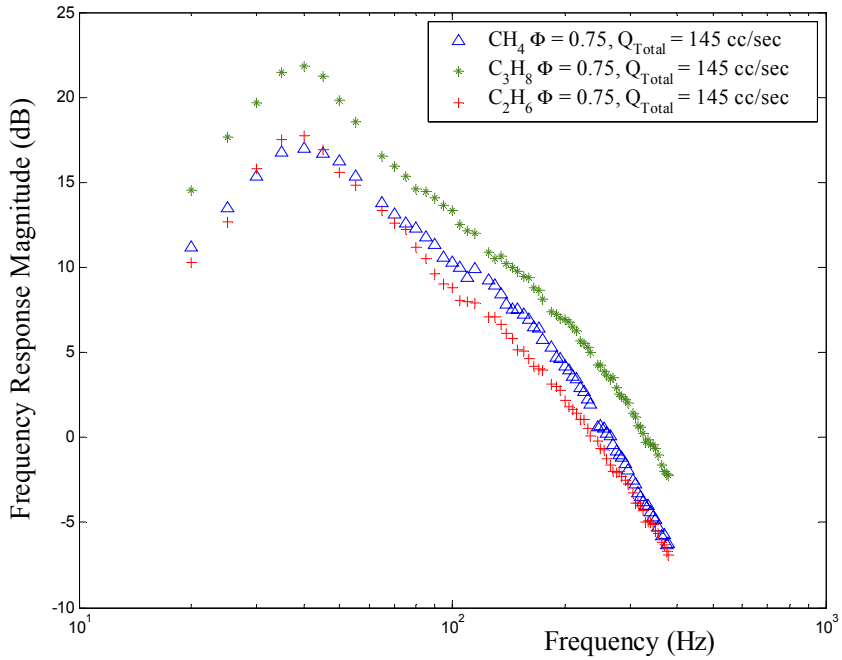

Figure 7.11: FRF (magnitude) for $Q_{Total} = 145$ cc/sec and $\Phi = 0.75$

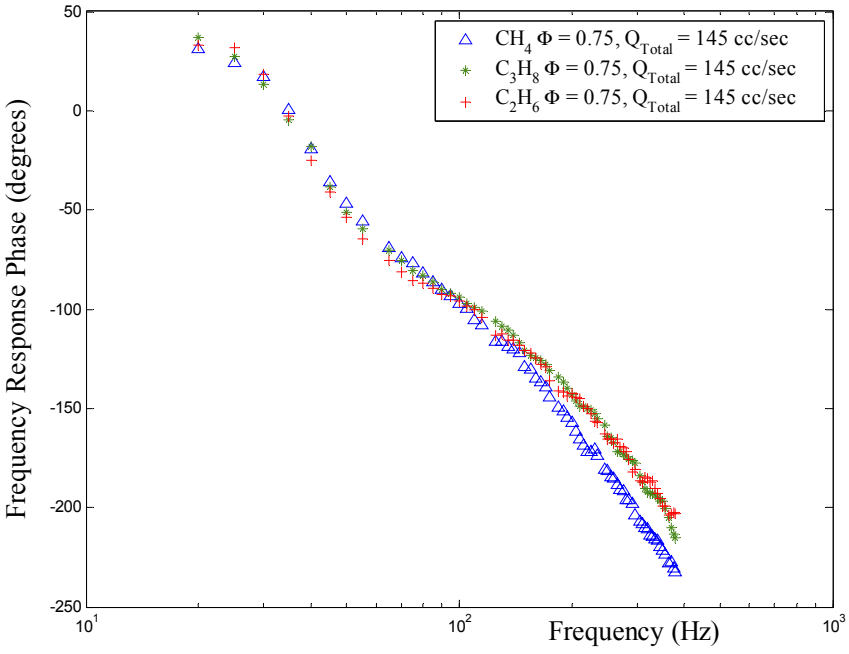

Figure 7.12: FRF (phase) for $Q_{Total} = 145$ cc/sec and $\Phi = 0.75$

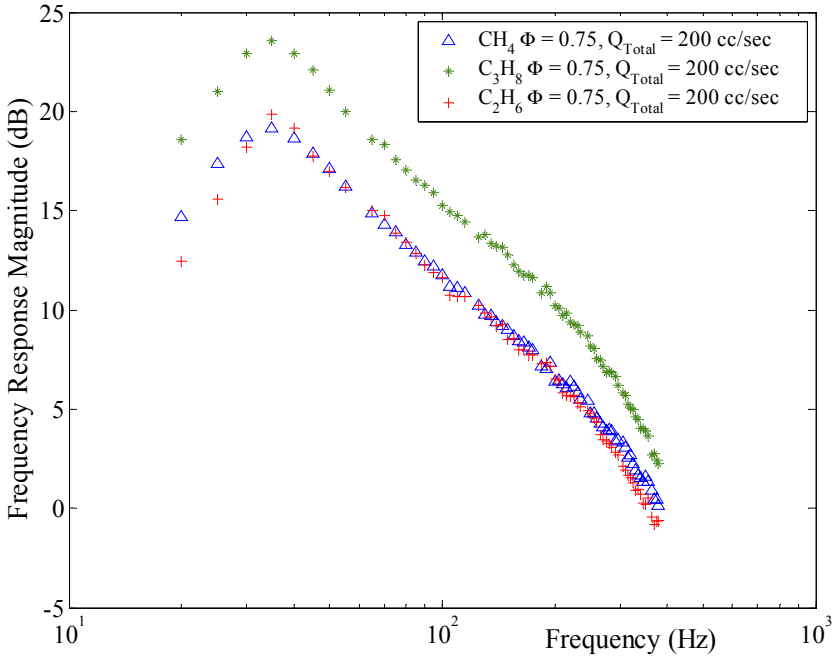

Figure 7.13: FRF (magnitude) for $Q_{Total} = 200$ cc/sec and $\Phi = 0.75$

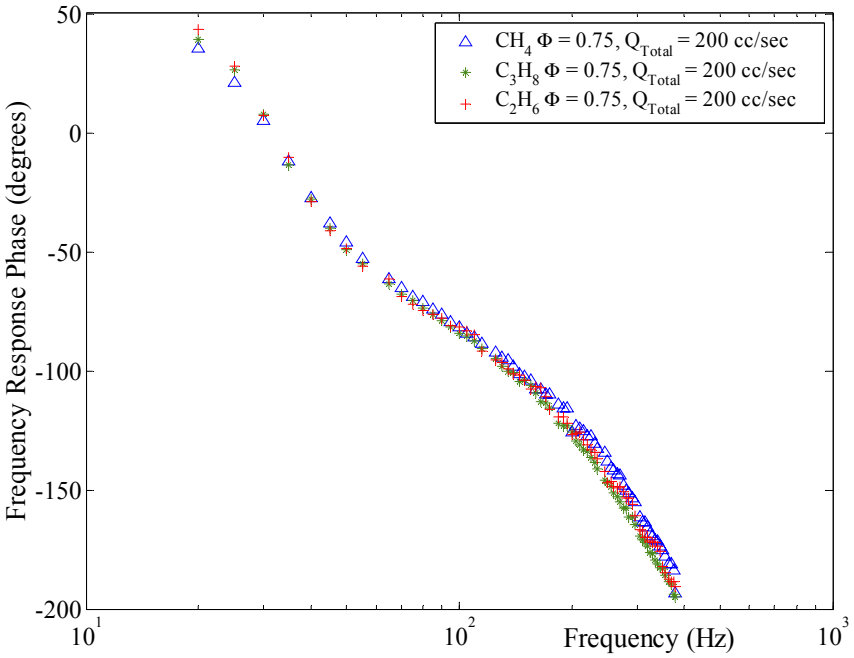

Figure 7.14: FRF (phase) for $Q_{Total} = 200$ cc/sec and $\Phi = 0.75$

the entire bandwidth while the phase exhibited by propane flames becomes almost identical to that of methane flames.

These observations indicate that at higher Φ of about 0.75, switching from methane to ethane air flames in most cases would have no effect on the thermo-acoustic instabilities. For intermediate equivalence ratios such as $\Phi = 0.65$, the marginally stable system could be made unstable by burning ethane due to slightly higher gain and small changes in phase. The likelihood of such an occurrence is greater for systems that exhibit marginal stability at frequencies within the range of 35-180 Hz. Changing fuels from methane to propane at higher equivalence ratios will increase the chances of occurrence of thermo-acoustic instabilities, purely due to an increase in dynamic gain. Thus, marginally stable systems burning methane as fuel will demonstrate thermo-acoustic instabilities upon burning propane.

7.2 Comparison of the Reduced Order Models

The results of the reduced order models discussed in Chapter 6 showed that all the three fuels had a similar dynamic behavior with regard to the dominant physical parameters. Yet, the presentation in Section 7.1 shows that when compared to each other, the three fuels have different dynamic characteristics. To improve upon the understanding of their dynamic behavior, the two resonant responses for all the three fuels are compared here and inferences are drawn with regard to their effects on the dynamic systems.

7.2.1 1^{st} Resonant Response

Figure 7.15 shows the 1^{st} resonant response for all the three fuels plotted on the 's plane'. The plot demonstrates two clusters of data, one for the 1^{st} resonant response of methane flames and the other for the 1^{st} resonant response of ethane and propane flames. The resonant frequency for propane and ethane flames is higher than that for methane flames, while the methane flames exhibit greater ζ as compared to ethane and propane flames. The frequency

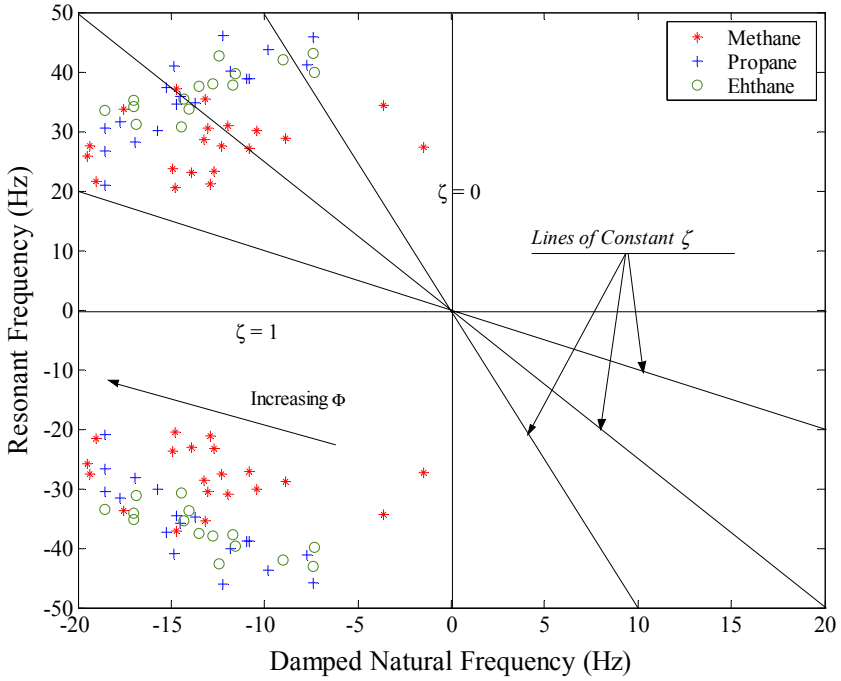

Figure 7.15: Phase plane for the 1^{st} resonant response

band in which the 1^{st} resonant response varies is largest for propane flames and smallest for methane flames. The variation in the resonant frequency of the 1^{st} resonant response indicates that it is not limited by the thermal capacity of the honeycomb, but is controlled by the dynamics of the combustion process that manifests as flame speed oscillations. Never the less, it is still a heat transfer driven low frequency oscillation of the flame speed that could be termed as the thermo-diffusive instability.

The damping ratio for all the data sets was plotted as a function of $\frac{dT}{dx}$ in Figure 7.16. It is noted that the data once again falls into two categories, one for methane flames and the other for propane and ethane flames. For the same heat transfer potential available, methane flames exhibit a higher damping ratio as compared to ethane and propane flames. This also indicates that the damping ratio is not only dependent on the heat transfer potential, but also on some other physical parameter which dominates the 1^{st} resonant response. Interestingly enough, the laminar flame speed which has been associated with the 1^{st} resonant response is

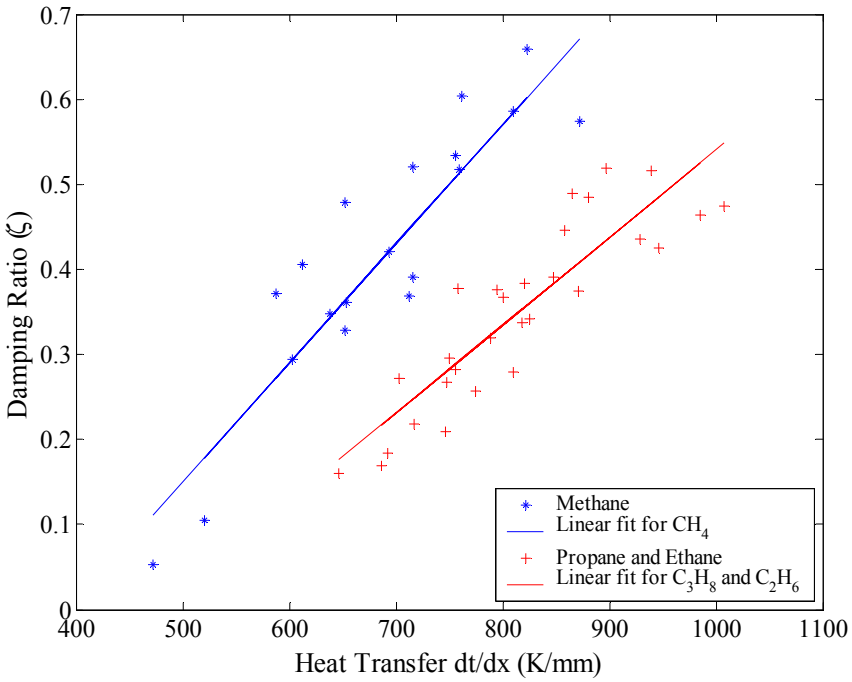

Figure 7.16: Dependence of ζ of the 1^{st} resonant response on the heat transfer potential

almost the same for both propane and ethane flames but is quite different from the methane flames. Thus, clustering of the data for ethane and propane flames into a region distinct from where the methane flame data resides, in both Figure 7.15 and Figure 7.16, further substantiates the conclusion that the 1^{st} resonant response represents the dynamic of flame speed oscillations.

7.2.2 2^{nd} Resonant Response

To compare the 2^{nd} resonant response of the three fuels, they were plotted together on the 's plane' and are shown in shown in Figure 7.17. Barring some scatter, the data could be considered to lie on two distinct damping ratio lines irrespective of the fuel. This is indicative of two dominant heat release mechanisms on either side of a threshold flame temperature. These dominant reactions do not distinguish between the types of fuel and

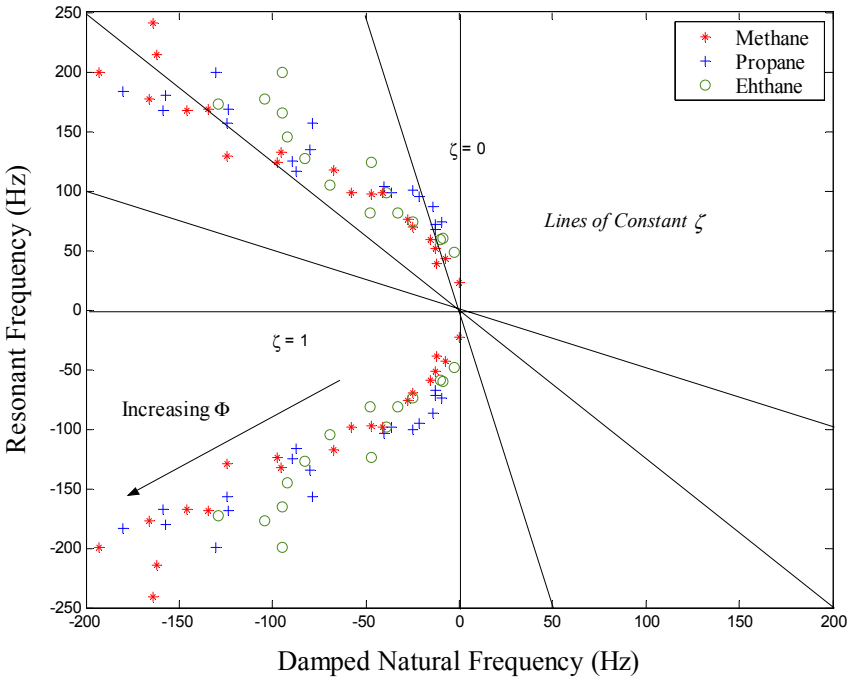

Figure 7.17: Phase plane for the 2^{nd} resonant response

thus are probably the chain propagating type of reactions that are expected to be common to the three fuels. A close examination of Figure 7.17 along with the 2^{nd} resonant response data from Appendix D shows that for similar conditions of Q_{Total} and Φ, ethane exhibits the lowest resonant frequency while methane has the highest resonant frequency. This indicates that the ethane flames were stabilized with the least flame temperature, while methane flames had the highest flame temperature. The above conclusion is verified by comparing the computed flame temperatures that are tabulated in Appendix D.

The resonant frequencies of the 2^{nd} resonant response were plotted as function of flame temperature and are shown in Figure 7.18. The data shows that the three fuels exhibit their own distinct exponential fits between the resonant frequency and the flame temperature. The three fits seem to merge at higher flame temperatures and spread apart at the lower range of flame temperatures. This behavior indicates that at higher equivalence ratios which generate high flame temperatures, the 2^{nd} resonant response is almost independent of the

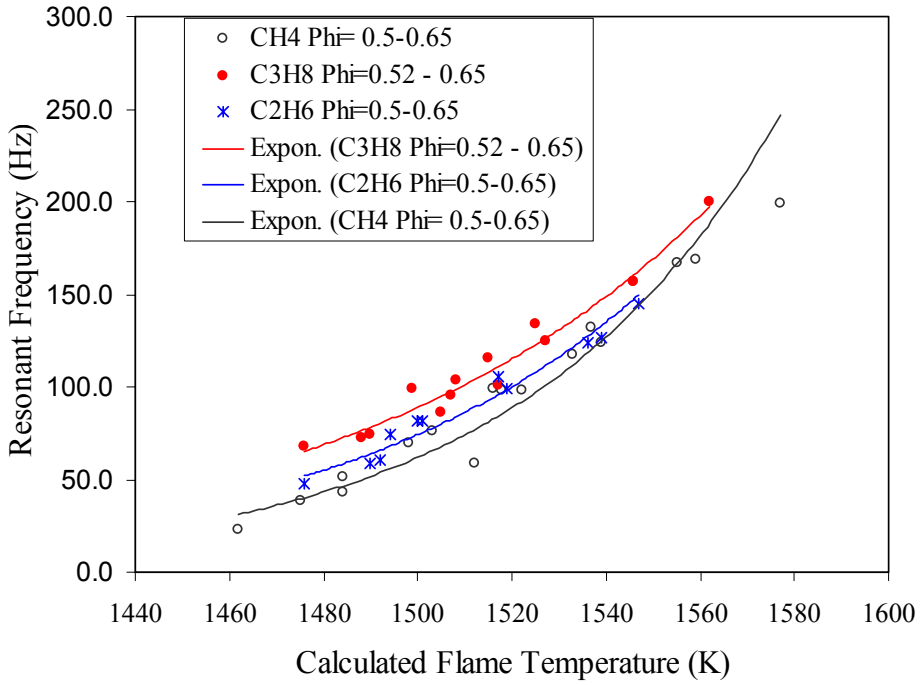

Figure 7.18: Frequencies of the 2^{nd} resonant response plotted as a function of flame temperature

fuel composition being burnt. But at lower equivalence ratios that are responsible for the low flame temperatures, injection of propane or ethane into methane flames will increase the bandwidth of the dynamic flame response by 30-40 Hz. This could increase the susceptibility of the combustion process to thermo-acoustic instabilities.

The above conclusion should be considered along with the fact that the prediction of the 2^{nd} resonant response, based on the experimental and the modeling procedures, has an error margin of ± 2 Hz and that the flame temperatures as predicted by the 'Premix' code could deviate from the actual flame temperature. However, the deviation in the prediction of the flame temperature is expected to be consistent for all the conditions. Thus, inaccuracies in the predicted flame temperatures would not effect the relative spacing between the curve fits of the three fuels, as seen in Figure 7.18. The error in the prediction of the 2^{nd} resonant response could reduce by 4 Hz the differential by which propane and ethane enhance the bandwidth of methane flames.

In summary of the fuel composition effects it is concluded that At $\Phi \leq 0.60$, the composition of the fuel being burnt plays an important role in defining the dynamics of the chemical kinetics, and thus the stability of the combustion system. At $\Phi > 0.60$, changes in fuel composition have negligible effect on the dynamics of chemical kinetics involved. However, the dynamic stability of the combustion system could still be affected via the dynamic gain.

7.3 Effect of Fuel Change on the Performance of the Rijke Tube

The Rijke tube described in Chapter 6 was fired using the same three fuels tested on the flat flame burner, to study the dynamic response of its operation. The study was conducted to support the discussions of Section 7.1 and Section 7.2. Experiments were conducted at

a. Conditions of equal mean energy content of fuel-air mixture and $\Phi = 0.5$
b. Total flow of 140 cc/sec and $\Phi = 0.5$
c. Total flow of 140 cc/sec and $\Phi = 0.55$
d. Total flow of 180 cc/sec and $\Phi = 0.55$

The power spectrum of the dynamic pressure trace while burning the three different fuels is shown in Figure 7.19 through Figure 7.22. Figure 7.19 shows the condition where the flow rates of the three fuels were adjusted to obtain the same mean energy content of the inlet mixture and $\Phi = 0.5$. Here, methane-air combustion is weakly unstable at about 178 Hz, but burning propane induces the Rijke tube to exhibit thermo-acoustic limit cycle. The difference in the two peaks is almost 50 dBV. On the other hand, burning ethane stabilizes the system by lowering the peak by about 10 dBV, but it also shows a weakly unstable broadband response at around 300 Hz. The behavior of both propane and ethane flames seen here reinforces the conclusions drawn in Section 7.1 and Section 7.2 that marginally stable systems, burning methane will exhibit instabilities when switched to propane. Also noted

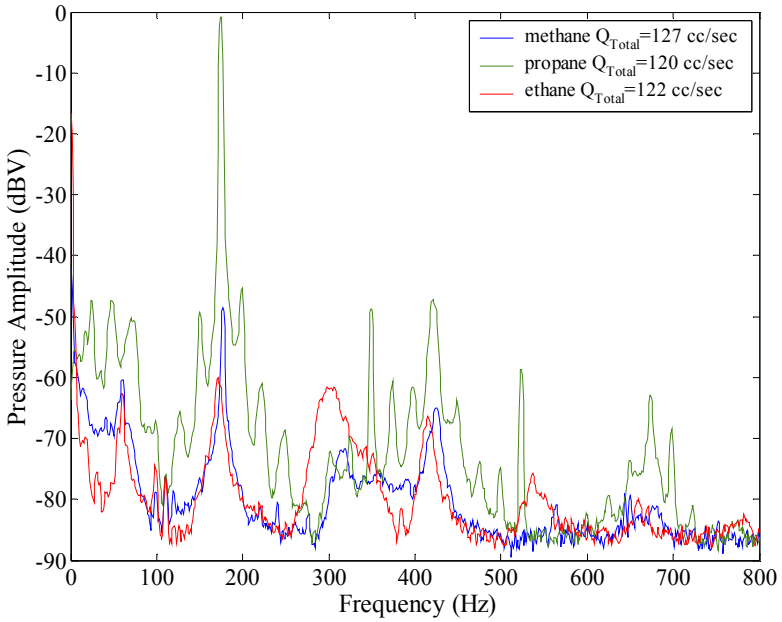

Figure 7.19: Power spectrum of the pressure trace in the Rijke tube combustor for $\Phi = 0.5$, and equal mean energy content

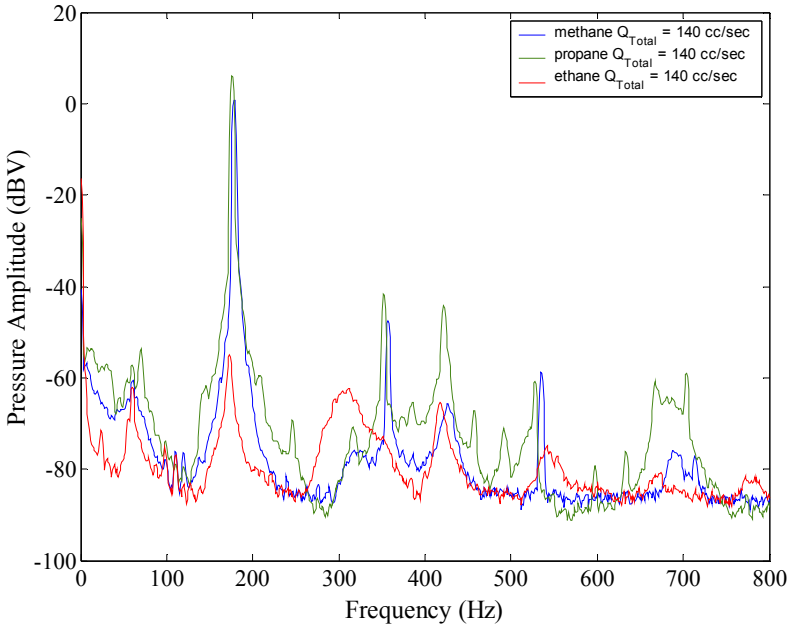

Figure 7.20: Power spectrum of the pressure trace in the Rijke tube combustor for $\Phi = 0.5$, and $Q_{Total} = 140$ cc/sec

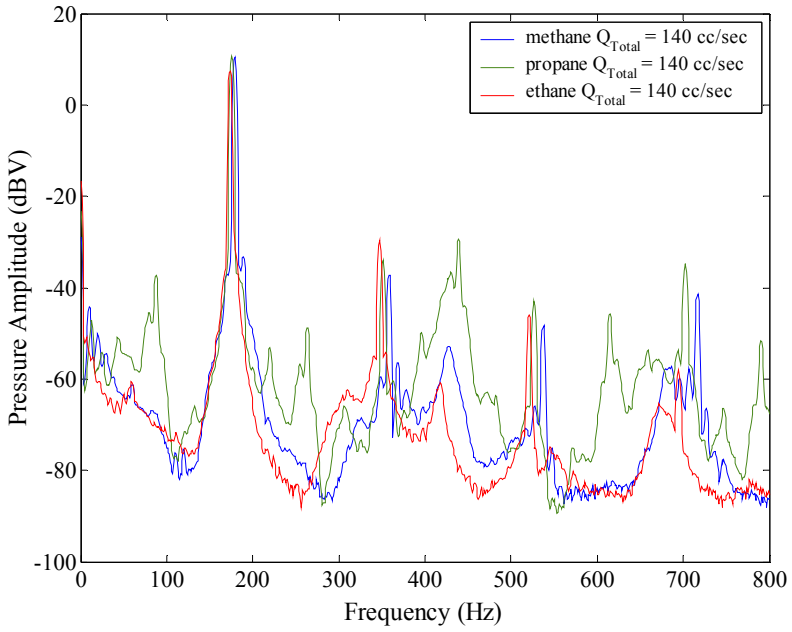

Figure 7.21: Power spectrum of the pressure trace in the Rijke tube combustor for $\Phi = 0.55$, and $Q_{Total} = 140$ cc/sec

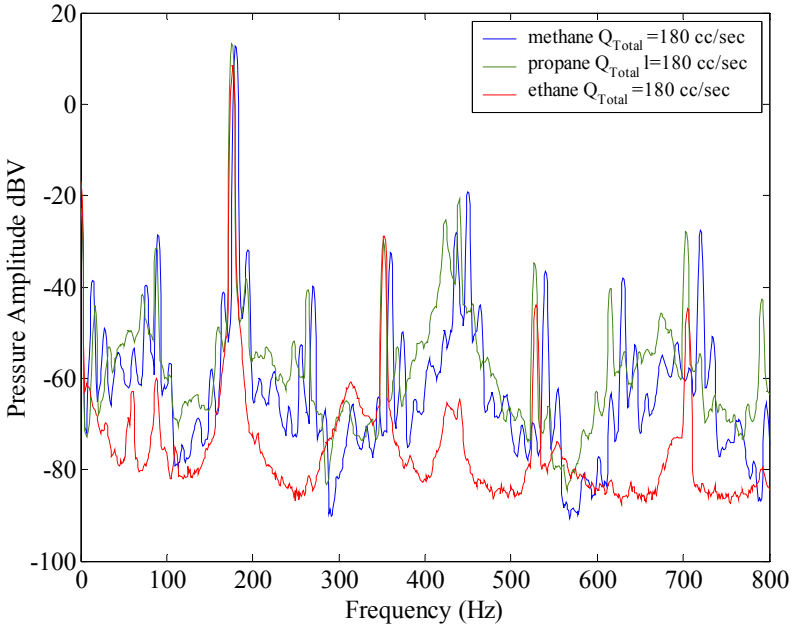

Figure 7.22: Power spectrum of the pressure trace in the Rijke tube combustor for $\Phi = 0.55$, and $Q_{Total} = 180$ cc/sec

in Figure 7.19 are the amplitude modulating side-bands exhibited by the power spectrum obtained from propane combustion. These side-bands correlate to the 1^{st} resonant response.

Figure 7.20 shows the power spectrum of the pressure signal for $\Phi = 0.5$ and $Q_{Total} = 140$ cc/sec. The combustion with propane and methane exhibit limit cycle behavior, but the amplitude of the limit cycle while burning methane is lower than that achieved while burning propane combustion by about 6 dBV. Ethane combustion, on the other hand still exhibits a weakly unstable system. Figure 7.21 shows the power spectrum of the pressure trace for $Q_{Total} = 140$ cc/sec and $\Phi = 0.55$, while Figure 7.22 shows the power spectrum of the pressure trace for $Q_{Total} = 180$ cc/sec and $\Phi = 0.55$. In both cases, the amplitude of the limit cycle is the same for both methane and propane indicating that the saturation mechanism for both the fuels is probably the same. Ethane exhibits the limit cycle amplitude of about 4 dBV below the other two. Both ethane and propane flames exhibit a limit cycle at a frequency which is about 4 Hz lower than that for methane flames. Since the limit cycling frequency of this Rijke tube is predominantly controlled by its acoustic characteristics, the shift in the limit cycling frequency is attributed to the fact that propane and ethane must be burning at lower flame temperatures than methane. Thus, using a Rijke tube that is designed to exhibit thermo-acoustic instabilities, the conclusions drawn about the dynamics of methane, ethane and propane flames have been shown to be correct.

The above discussions have conclusively shown that at ultra lean operating conditions, the chemical kinetics involved in the combustion process plays an important role in defining the stability of the combustion system. Thus, while developing active control methodologies for lean premixed combustion, the type of fuel being burnt and its composition needs to be accounted and closely monitored for dynamic changes. Furthermore the fuel used in the operation of a combustor should be changed only after evaluating it's impact on the stability of the combustor.